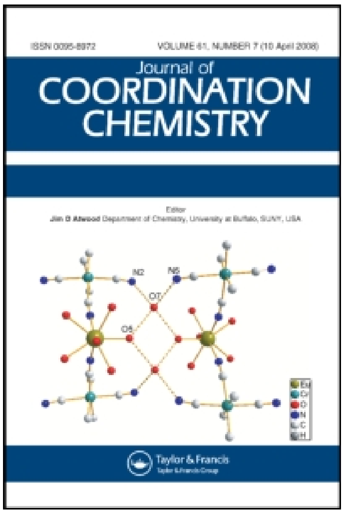

Journal of Coordination Chemistry
Publication details, including instructions for authors and subscription information:
http://www.informaworld.com/smpp/title~content=t713455674

Bis(2-Amino-5-bromopyrimidinium) Tetrahalometallates: Crystal structures of (2-amino-5-bromopyrimidinium)2 MCl_4 (M = Co, Zn)

Sebastian Andrews[a]; Jessica Corwin[a]; Brian Landry[a]; Michaela Martin[a]; Katherine Parnass[a]; Andrew Suen[a]; Mark M. Turnbull[a]; Ryan T. Schneider[b]; Christopher P. Landee[b]; Firas F. Awwadi[c]
[a] Carlson School of Chemistry and Biochemistry, Clark University, Worcester, MA 01610, USA [b] Department of Physics, Clark University, Worcester, MA 01610, USA [c] Department of Chemistry, Washington State University, Pullman, WA 99164, USA

To cite this Article Andrews, Sebastian , Corwin, Jessica , Landry, Brian , Martin, Michaela , Parnass, Katherine , Suen, Andrew , Turnbull, Mark M. , Schneider, Ryan T. , Landee, Christopher P. and Awwadi, Firas F.(2006) 'Bis(2-Amino-5-bromopyrimidinium) Tetrahalometallates: Crystal structures of (2-amino-5-bromopyrimidinium)2 MCl_4 (M = Co, Zn)', Journal of Coordination Chemistry, 59: 13, 1451 — 1465

To link to this Article: DOI: 10.1080/00958970600559385
URL: http://dx.doi.org/10.1080/00958970600559385

Journal of Coordination Chemistry
Vol. 59, No. 13, 10 September 2006, 1451–1465

Taylor & Francis
Taylor & Francis Group

Bis(2-Amino-5-bromopyrimidinium) Tetrahalometallates: Crystal structures of (2-amino-5-bromopyrimidinium)2 MCl$_4$ (M = Co, Zn)

SEBASTIAN ANDREWS†, JESSICA CORWIN†, BRIAN LANDRY†,
MICHAELA MARTIN†, KATHERINE PARNASS†, ANDREW SUEN†, MARK
M. TURNBULL*†, RYAN T. SCHNEIDER‡, CHRISTOPHER P. LANDEE‡ and
FIRAS F. AWWADI§

†Carlson School of Chemistry and Biochemistry, Clark University,
Worcester, MA 01610, USA
‡Department of Physics, Clark University, Worcester, MA 01610, USA
§Department of Chemistry, Washington State University, Pullman, WA 99164, USA

(*Received 15 September 2005*)

The reactions of metal(II) chlorides and bromides with 2-amino-5-bromopyrimidine (2-abpm) in neutral and acidic solution were investigated. The reaction with $ZnCl_2$, $ZnBr_2$, $CoCl_2$, $CoBr_2$ and $MnCl_2$ in acidic nitromethane solution gave complexes of the formula $(2\text{-abpmH})_2MX_4$ (**1**, M = Zn, X = Cl; **2**, M = Zn, X = Br; **3**, M = Co, X = Cl; **4**, M = Co, X = Br; **5**, M = Mn, X = Cl). Crystals of **1** and **3** suitable for single crystal X-ray diffraction were obtained. Crystal data: For (**1**): triclinic, P-1, $a = 6.2485(13)$, $b = 9.0520(14)$, $c = 15.334(4)$ Å, $\alpha = 94.81(2)$, $\beta = 95.224(17)$, $\gamma = 98.027(17)°$, $V = 851.1(3)$ Å^3, $Z = 2$, $R = 0.0596$ for $[|I| \geq 2\sigma(I)]$. For (**3**): triclinic, P-1, $a = 6.2438(13)$, $b = 9.0597(15)$, $c = 15.318(3)$ Å, $\alpha = 94.749(18)$, $\beta = 95.343(15)$, $\gamma = 98.021(17)°$, $V = 850.2(3)$ Å^3, $Z = 2$, $R = 0.0452$ for $[|I| \geq 2\sigma(I)]$. Variable temperature magnetic susceptibility data indicates weak antiferromagnetic interactions in the cobalt and manganese complexes.

Keywords: Tetrahalometallates; 2-Amino-5-bromopyrimidine; Crystal structure; Hydrogen

1. Introduction

Coordination complexes and salts of nitrogen heterocycles with 2+ transition metal halides exhibit a variety of structures and packing motifs. We have recently studied a series of manganese [1], cobalt [2], nickel [2] and copper [3] complexes of 2-aminopyrimidine and were interested in extending this study to substituted 2-aminopyrimidines to determine how the change in organic cation would affect the packing of tetrahalometallate anions. Pyrimidine moieties are well known in a variety

---

*Corresponding author. Email: MTurnbull@clarku.edu

Journal of Coordination Chemistry
ISSN 0095-8972 print: ISSN 1029-0389 online © 2006 Taylor & Francis
DOI: 10.1080/00958970600559385

of biologically active compounds and 2-amino-5-bromopyrimidine is a common starting material [4] which has been used in the synthesis of rodenticides [5], Fab I inhibitors [6], anti-microbial compounds [7] and phosphodiesterase inhibitors [8]. The activity of many bioactive materials is related to their structure and ability to form hydrogen bonds with substrate molecules [9]. The most common packing structure in 2-aminopyrimidine compounds is that of hydrogen-bonded dimers, leading to the formation of chains and sheets within the lattice structure [10, 11]. The formation of these hydrogen-bonded dimers can be inhibited by the presence of water molecules, or by coordination of the pyrimidine nitrogen atoms [12–14]. Although 2-amino-5-bromopyrimidine (2-abpm) has been used to prepare substituted 2-aminopyrimidines for the generation of supramolecular lattice structures controlled principally by hydrogen bonding [15], little is known of the coordination chemistry and packing structures of 2-amino-5-bromopyrimidine itself [3, 14]. Therefore, we undertook the preparation of a number of transition metal complexes containing the 2-abpm moiety with the intent of analyzing the differences that inclusion of the additional bromine atom may have on the structure and packing of the complexes. We report here the synthesis of a family of 2-amino-5-bromopyrimidinium complexes and the crystal structures of $(2\text{-abpmH})_2MCl_4$ [M = Zn, Co).

2. Experimental

Metal salts and acids, nitromethane and 2-aminopyrimidine were purchased from Aldrich Chemical. All materials were used as received. No attempts were made to maximize yields from crystallizations. 2-Amino-5-bromopyrimidine was prepared according to the method of Cross *et al.* [16]. Infrared spectra were recorded as KBr pellets (m = medium, s = strong, br = broad, mu = multiple) on a PE-1600 or Paragon 500 infrared spectrophotometer and referenced to polystyrene. Room temperature magnetic susceptibility measurements were made on a Johnson-Matthey Susceptibility balance. Variable temperature magnetic susceptibility measurements were made on powdered samples loaded in #3 gelatin capsules on a Quantum Design MPMS SQUID Magnetometer and corrected for temperature independent paramagnetism. Diamagnetic corrections were made using Pascal's contants.

Bis(2-amino-5-bromopyrimidinium) tetrachlorozincate(II), **1** – $ZnCl_2$ (0.069 g, 0.51 mmol) was added to 10 mL of nitromethane along with two drops of concentrated HCl and the solution heated to near boiling. 2-Amino-5-bromopyimidine (0.174 g, 1.00 mmol) was added to 10 mL of nitromethane, acidified with 5 drops of concentrated HCl and heated to near boiling. The pyrimidine mixture was then added to the $ZnCl_2$ mixture and the resulting mixture heated until solution was nearly complete. The hot solution was decanted from the residual solid and allowed to cool and evaporate slowly in air over the course of one week, resulting in the formation of colorless, rod-shaped crystals. The crystals were collected by vacuum filtration, washed with cold nitromethane and allowed to air dry to give 0.170 g (30%). Mp = 221–4°C. Anal. Calcd for $C_8H_{10}N_6Cl_4ZnBr_2$: C, 17.24; H, 1.81; N, 15.08; found: C, 16.96; H, 2.02; N, 14.92. IR (KBr) – ν 3329s, 3222m, 3152s, 3067s, 3012m, 1676vs, 1614s, 1374m, 1202m, 808w, 770w cm^{-1}.

Bis(2-amino-5-bromopyrimidinium) tetrabromozincate(II), **2** – $ZnBr_2$ (0.067 g, 0.30 mmol) and 2-amino-5-bromopyrimidine (0.105 g, 0.60 mmol) were added to 4 mL of nitromethane and heated for several minutes. The solution was acidified with 2 drops of concentrated HBr generating an immediate precipitate. The hot mixture was filtered and the precipitate washed with cold nitromethane and allowed the air dry. [This initial precipitate was characterized as 2-amino-5-bromopyrimidinium bromide by comparison with a sample made by independent synthesis]. After removal of the initial precipitate, the filtrate was allowed to cool. This sample proved to be 2-amino-5-bromopyrimidinium bromide by comparison with a sample made by independent synthesis. The filtrate was allowed to cool and evaporate slowly in air over the course of one week, resulting in the formation of thin, transparent, rod-shaped crystals. The crystals were collected by vacuum filtration, washed with cold nitromethane and allowed to air dry to give 0.045 g (21%). Mp = 210–212°C. Anal. Calcd for $C_8H_{10}N_6CoBr_6$: C, 13.07; H, 1.37; N, 11.43; found: C, 13.45; H, 1.56; N, 11.84. IR (KBr) – ν 3392m, 3350s, 3284m, 2093m, 1676vs, 1642s, 1608s, 1555s, 1484s, 1372m, 1200m, 786s cm^{-1}.

Bis(2-amino-5-bromopyrimidinium) tetrachlorocobaltate(II), **3** – $CoCl_2 \cdot 6H_2O$ (0.24 g, 0.10 mmol) and 2-amino-5-bromopyrimidine (0.035 g, 0.20 mmol) were combined in 2.5 mL of nitromethane along with 11 drops of concentrated HCl. The mixture was then heated slowly to near boiling adding nitromethane dropwise until solution was nearly complete. The supernatant liquid was decanted from the trace insoluble residue and allowed to cool resulting in the formation of small, blue crystals. The crystals were collected by vacuum filtration, washed with cold nitromethane and allowed to air dry to give 0.030 g (54%). Mp = 220-2(d). Anal. Calcd for $C_8H_{10}N_6Cl_4CoBr_2$: C, 17.44; H, 1.83; N, 15.26; found: C, 17.81; H, 2.02; N, 15.10. IR (KBr) – ν 3327m, 3160m, 3069m, 1676vs, 1612s, 1374m, 1201m, 808w, 769 cm^{-1}. $\chi_{mol} = 8.49 \times 10^{-3}$ cgs (295 K).

Bis(2-amino-5-bromopyrimidinium) tetrabromocobaltate(II), **4** – $CoBr_2$ (0.45 g, 1.35 mmol) and 2-amino-5-bromopyrimidine (0.348 g, 2.00 mmol) were combined in 10 mL of nitromethane and 5 drops of concentrated HBr added. The mixture was heated to near boiling adding nitromethane dropwise until virtually all material had dissolved. Addition of 2 more drops of concentrated HBr gave a dark blue solution. The flask was capped and allowed to cool to room temperature overnight, resulting in blue crystals. The crystals were collected by vacuum fitration, washed with cold nitromethane and dried under vacuum to give 0.0535 g (74%). The compound is hygroscopic, especially so while still wet, turning pink, presumably due to hydration of the cobalt ion. Mp = 198–201°C (d). IR (KBr) – ν 3300 br s (H_2O), 1670vs, 1612s, 1375m, 1340m, 12692, 1217w, 1018m, 808m, 769m, 598 cm^{-1}. $\chi_{mol} = 9.87 \times 10^{-3}$ cgs (295 K).

Bis(2-amino-5-bromopyrimidinium) tetrachloromanganate(II), **5** – $MnCl_2 \cdot 4H_2O$ (0.059 g, 0.30 mmol) and 2-amino-5-bromopyrimidine (0.104 g, 0.60 mmol) were combined in 9 mL of nitromethane and 6 drops of concentrated HCl added. The mixture was heated to near boiling resulting in a pale yellow solution. The solution was allowed to cool giving pale yellow crystals. The crystals were collected by vacuum fitration, washed with cold nitromethane and allowed to air dry to give 0.135 g (82%). Anal. Calcd for $C_8H_{10}N_6Cl_4MnBr_2$: C, 17.55; H, 1.83; N, 15.36; found: C, 17.42; H, 1.89; N, 15.31. IR (KBr) – ν 3195s, 3074s, 3056s, 1676vs, 1609s, 1376m, 1344m, 1217m, 784w, 770m, 597br s cm^{-1}. $\chi_{mol} = 1.54 \times 10^{-2}$ cgs (294 K).

2.1. *X-ray structure determination*

Data collections for the tetrachlorometallates **1** and **3** were carried out on a Siemens $P2_1$ diffractometer upgraded to P4 employing Mo-Kα radiation ($\lambda = 0.71073$) and a graphite monochromator. Data collection via ω-scans and cell refinement were performed using Bruker XSCANS software [17] and data reduction were performed using Bruker SHELXTL software [18]. Absorption corrections were made via ψ-scans. Structures were solved using the heavy atom Patterson method [SHELXS-97] and full-matrix least-squares refinement was done via SHELXL-97 [19]. Aromatic hydrogen atoms were refined via a riding model with fixed isotropic U's. The hydrogen atoms bonded to nitrogen atoms were located in the difference maps and allowed to refine with fixed isotropic U's. Crystallographic data may be found in table 1. Selected bond lengths and angles are given in table 2. Hydrogen bonds are listed in table 3.

Table 1. Crystal data and structure refinement for **1** and **3**.

	1	**3**
Empirical formula:	$C_8H_{10}Br_2Cl_4N_6Zn$	$C_8H_{10}Br_2Cl_4CoN_6$
Formula weight	557.21	550.77
Crystal system	Triclinic	Triclinic
Crystal habit	Plate	Block
Space group	P-1	P-1
Unit cell dimensions (Å):		
a (Å)	6.2485(13)	6.2438(13)
b (Å)	9.0520(14)	9.0597(15)
c (Å)	15.334(4)	15.318(3)
α (°)	94.81(2)	94.749(18)
β (°)	95.224(17)	95.343(15)
γ (°)	98.027(17)	98.021(17)
Volume (Å^3)	851.1(3)	850.2(3)
Z	2	2
Density (calcd) (Mg m^{-3})	2.174	2.151
Size(mm)	$0.5 \times 0.25 \times 0.1$	$0.5 \times 0.3 \times 0.2$
$F(000)$	536	530
μ(mm^{-1})	6.765	6.337
Data collection:		
Temperature (K)	295(2)	295(2)
Max., min. transmission	0.8735, 0.2241	0.8055, 0.3022
Reflections collected	3770	3783
Independent reflections	2899	2910
θ range (°)	2.53 to 24.73	2.28 to 24.76
Range h, k, l	$-7 \leq h \leq 1$ $-10 \leq k \leq 10$ $-18 \leq l \leq 18$	$-1 \leq h \leq 7$ $-10 \leq k \leq 10$ $-18 \leq l \leq 18$
Refinement:		
Data/restraints/parameters	2899/0/208	2910/0/209
Goodness-of-fit on F^2	1.005	1.034
Final R indices [$I > 2\sigma(I)$]		
R_1	0.0596	0.0452
wR_2	0.1395	0.1006
R indices (all data)		
R_1	0.0911	0.0696
wR_2	0.1573	0.1115
Largest difference peak (e Å^{-3})	0.911	0.639
Largest difference hole (e Å^{-3})	−0.898	−0.707

Table 2. Metal halide bond lengths (Å) and angles (°) for **1** and **3**.

Bond lengths	1	**3**	Bond angles	1	**3**
M–Cl1	2.268(2)	2.2708(18)	Cl1–M–Cl2	114.16(10)	114.85(7)
M–Cl2	2.278(2)	2.2755(16)	Cl1–M–Cl3	104.92(9)	104.25(6)
M–Cl3	2.275(2)	2.2818(17)	Cl1–M–Cl4	107.50(9)	106.99(7)
M–Cl4	2.282(2)	2.2835(17)	Cl2–M–Cl3	109.59(8)	109.58(6)
			Cl2–M–Cl4	107.73(8)	107.56(6)
			Cl3–M–Cl4	113.04(9)	113.75(7)
N1–C2	1.356(11)	1.338(8)	C6–N1–C2	122.4(7)	122.8(5)
C2–N2	1.306(12)	1.314(9)	N1–C2–N2	119.8(8)	120.4(5)
C2–N3	1.349(10)	1.356(7)	N1–C2–N3	120.1(8)	120.6(5)
N3–C4	1.325(10)	1.310(7)	N2–C2–N3	120.1(9)	119.0(6)
C4–C5	1.377(12)	1.389(8)	C2–N3–C4	117.9(7)	116.9(5)
C5–C6	1.357(11)	1.360(8)	N3–C4–C5	123.1(7)	124.4(5)
C5–Br1	1.885(8)	1.875(6)	C4–C5–C6	118.9(8)	117.2(6)
C6–N1	1.352(11)	1.341(8)	C4–C5–Br1	120.3(6)	120.8(4)
			C6–C5–Br1	120.8(7)	122.0(5)
			C5–C6–N1	117.6(8)	118.2(6)
N11–C12	1.356(13)	1.352(9)	C16–N11–C12	122.2(8)	121.4(6)
C12–N12	1.293(13)	1.304(9)	N11–C12–N12	119.8(9)	119.4(6)
C12–N13	1.352(12)	1.343(8)	N11–C12–N13	119.0(8)	120.6(6)
N13–C14	1.319(11)	1.319(8)	N12–C12–N13	121.2(10)	120.0(7)
C14–C15	1.376(13)	1.377(9)	C12–N13–C14	118.8(8)	117.6(6)
C15–C16	1.349(13)	1.346(9)	N13–C14–C15	122.8(9)	123.5(6)
C15–Br11	1.890(8)	1.886(6)	C14–C15–C16	118.1(8)	117.9(6)
C16–N11	1.339(12)	1.345(8)	C14–C15–Br11	120.7(7)	121.2(5)
			C16–C15–Br11	121.2(7)	120.9(5)
			C15–C16–N11	119.0(9)	119.0(6)

Full crystallographic details, atomic coordinates and thermal parameters, full tables of bond lengths and angles, and anisotropic thermal parameters are available [20].

3. Results

3.1. *Synthesis*

Complexes **1–5** were prepared by reaction of the appropriate metal salt with HX and 2-abpm in hot nitromethane solution (scheme 1). The choice of solvent was made after many trials due to the poor solubility of 2-abpm and 2-abpmH$^+$X$^-$ in most polar protic solvents (e.g. water, MeOH, EtOH) and the poor solubility of the metal salt in low polarity organic solvents (e.g. CH_2Cl_2, CH_3CN). In addition, the 2-abpmH+X-salts could only be isolated from solutions containing at least a two-fold excess of acid. Attempts to prepare samples in DMSO resulted in DMSO-solvates which decomposed on standing in air. The cobalt bromide complex, **4**, proved unusually hygroscopic compared to the other complexes. Cooling of the hot nitromethane solution in a sealed container gave microcrystals of **4**, but attempts to grow larger crystals through slow evaporation in air gave a pink oil, presumably a hydrated cobalt species. The dry solid is moderately stable to air, but color changes at the surface of the crystals (blue to pink)

Table 3. Hydrogen bonds for **1** and **3** [Å and °].

For **1**

D–H···A	d(D–H)	d(H···A)	d(D···A)	∠(DHA)
N(2)–H(2A)···N(3)#1	0.83(12)	2.33(12)	3.150(12)	174(11)
N(12)–H(12A)···N(13)#2	0.87(12)	2.26(13)	3.123(13)	176(11)
N(1)–H(1)···Cl(2)	0.82(9)	2.48(9)	3.231(7)	154(9)
N(2)–H(2B)···Cl(2)	0.78(10)	2.65(11)	3.366(10)	153(11)
N(2)–H(2B)···Cl(2)#3	0.78(10)	2.82(11)	3.278(8)	120(10)
N(11)–H(11)···Cl(1)#4	0.79(10)	2.82(10)	3.476(8)	142(9)
N(12)–H(12B)···Cl(1)#4	0.92(12)	2.49(13)	3.353(11)	158(10)
N(12)–H(12B)···Cl(3)#4	0.92(12)	2.76(11)	3.244(9)	114(9)

Symmetry transformations used to generate equivalent atoms:
#1 $-x+2, -y+2, -z+1$ #2 $-x, -y, -z$ #3 $-x+2, -y+1, -z+1$ #4 $x-1, y, z$.

For **3**

D–H···A	d(D–H)	d(H···A)	d(D···A)	∠(DHA)
N(1)–H(1)···Cl(2)	0.74(6)	2.53(7)	3.229(5)	159(7)
N(2)–H(2A)···Cl(2)	0.87(7)	2.59(7)	3.375(6)	151(6)
N(2)–H(2A)···Cl(2)#1	0.87(7)	2.80(7)	3.278(6)	116(5)
N(2)–H(2B)···N(3)#2	0.64(8)	2.54(8)	3.139(8)	160(11)
N(11)–H(11)···Cl(1)#3	0.95(7)	2.62(7)	3.457(6)	147(5)
N(11)–H(11)···Cl(4)	0.95(7)	2.82(7)	3.437(6)	123(5)
N(12)–H(12A)···N(13)#4	1.10(8)	2.06(8)	3.120(9)	162(6)
N(12)–H(12B)···Cl(1)#3	0.69(8)	2.73(9)	3.340(7)	149(10)
N(12)–H(12B)···Cl(3)#3	0.69(8)	2.78(9)	3.250(7)	129(9)

Symmetry transformations used to generate equivalent atoms:
#1 $-x+2, -y+1, -z+1$ #2 $-x+2, -y+2, -z+1$ #3 $x-1, y, z$ #4 $-x, -y, -z$..

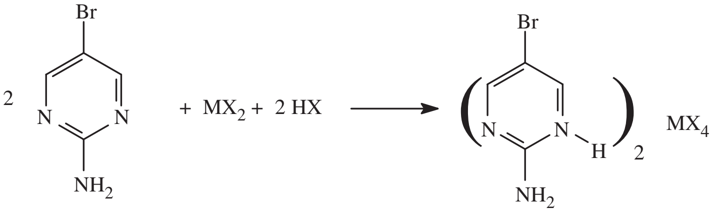

1, M = Zn, X = Cl; **2**, M = Zn, X = Br; **3**, M = Co, X = Cl
4, M = Co, X = Br; **5**, M= Mn, X= Cl

Scheme 1.

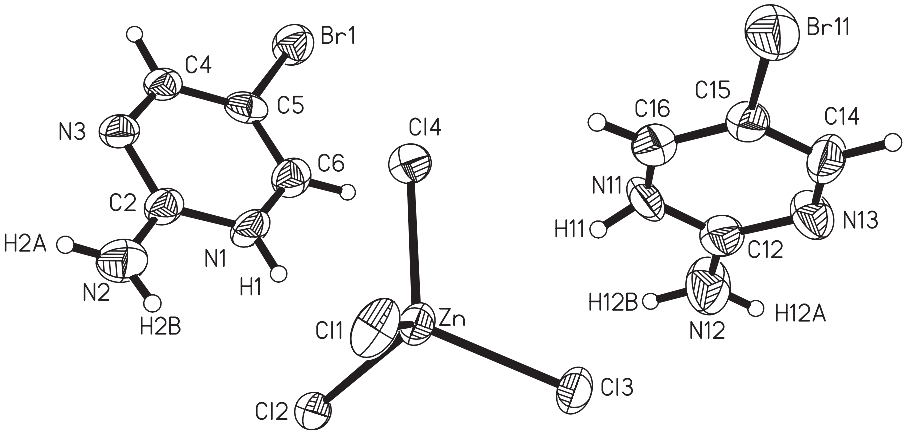

Figure 1. Thermal ellipsoid plot of **1** showing 50% probability ellipsoids. Hydrogens atoms are shown as spheres of arbitrary size and only those hydrogen atoms whose positions were refined are labeled.

could be observed after several minutes exposure. Samples for IR and magnetic susceptibility measurements were ground under an argon atmosphere, but still absorbed some moisture (clearly visible in the IR). The remaining compounds appear to be stable to air for extended periods of time. Attempts to prepare the corresponding compounds from $NiCl_2$, $NiBr_2$, $FeCl_2$ and $MnBr_2$ were unsuccessful in our hands, resulting in the isolation of the pyrimidine salt, 2-abpmHX (X = Cl, Br).

3.2. *X-Ray structures*

Crystals of **1** were grown by slow evaporation of a nitromethane solution. The asymmetric unit is shown in figure 1. The complex crystallizes in the triclinic space group P-1 with nearly tetrahedral coordination about the Zn ion (the mean trans angle [21] is 113.6(1)°). The zinc chlorine bond lengths are typical [22]. Corresponding bond lengths and angles in the two 2-abpmH rings are identical within experimental error and agree with those observed previously [3].

Each of the 2-abpmH rings forms an inversion related dimer via hydrogen bonding (see figure 2). These are [$R_2^2(8)$] systems, using Etter's notation [23] The lattice is further stabilized by hydrogen bonds between the pyrimidinium and amino hydrogen atoms and the chloride ions (see table 3).

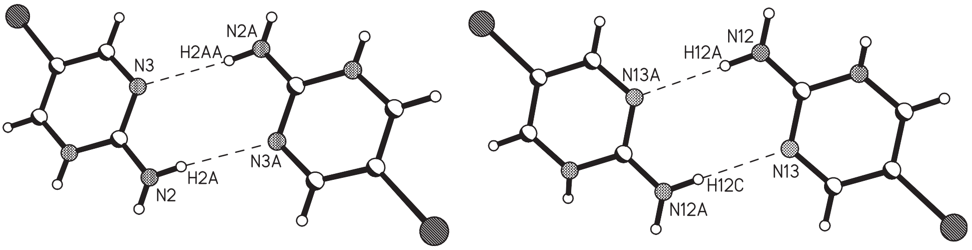

Figure 2. Packing diagram showing hydrogen bonding dimerization of the 2-abpmH moieties.

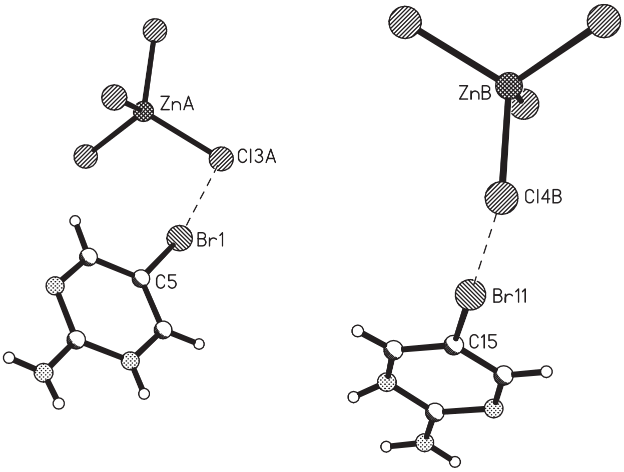

Figure 3. Packing diagram showing the halogen-halide interactions which aid in stabilizing the lattice (see text for interatomic distances and angles).

In addition, there are halogen-halide interactions between the 2-abpmH bromine atoms and the chloride ions [$d_{\mathrm{Br1}\cdots\mathrm{Cl3A}} = 3.540(2)$ Å, $\angle_{\mathrm{C5–Br1}\cdots\mathrm{Cl3A}} = 169.0(3)^\circ$, $\angle_{\mathrm{Br1}\cdots\mathrm{Cl3A–ZnA}} = 94.0(3)^\circ$; $d_{\mathrm{Br11}\cdots\mathrm{Cl4B}} = 3.383(2)$ Å, $\angle_{\mathrm{C15–Br11}\cdots\mathrm{Cl4B}} = 178.3(3)^\circ$, $\angle_{\mathrm{Br1}\cdots\mathrm{Cl3A–ZnA}} = 102.1(3)^\circ$; symmetry transformations: $\mathrm{A} = x-1,\ y+1,\ z$; $\mathrm{B} = -x+2,\ -y+1,\ -z$] (see figure 3).

The resulting overall packing structure is shown in figure 4. The $\mathrm{ZnCl_4^{2-}}$ ions and the 2-abpmH$^+$ dimers are stacked parallel to the *a*-axis of the crystal. The stacks are then interconnected into a three dimensional network via the hydrogen bonding and halide-halogen contacts.

Crystals of **3** were grown by cooling of a hot nitromethane solution. The asymmetric unit is shown in figure 5. The compound is isomorphous with **1**. The tetrahedral geometry about the cobalt ion is slightly more distorted than that observed for the zinc complex [mean trans angle = 114.3(1)°] and the cobalt chlorine bond lengths are again typical [2]. Corresponding bond lengths and angles in the two 2-abpmH rings in **3** are the same within experimental error and match those observed for **1**.

The hydrogen bonding network, including the formation of the [$\mathrm{R_2^2(8)}$] dimers, is the same as observed for **1** and the halogen-halide contacts are repeated as well [$d_{\mathrm{Br1}\cdots\mathrm{Cl3A}} = 3.527(2)$ Å, $\angle_{\mathrm{C5–Br1}\cdots\mathrm{Cl3A}} = 169.2(2)^\circ$, $\angle_{\mathrm{Br1}\cdots\mathrm{Cl3A–CoA}} = 94.6(2)^\circ$;

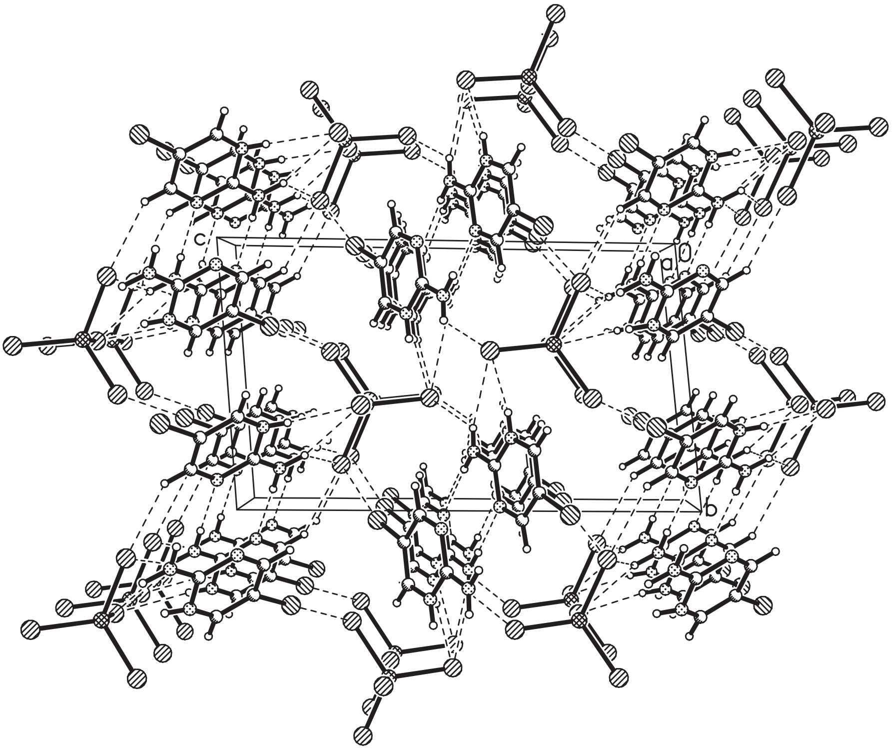

Figure 4. Packing diagram showing the stacking of the $ZnCl_4^{2-}$ ions and the 2-abpmH dimers viewed parallel to the *a*-axis. Dashed lines represent hydrogen bonds and short Br $\cdots$ Cl contacts.

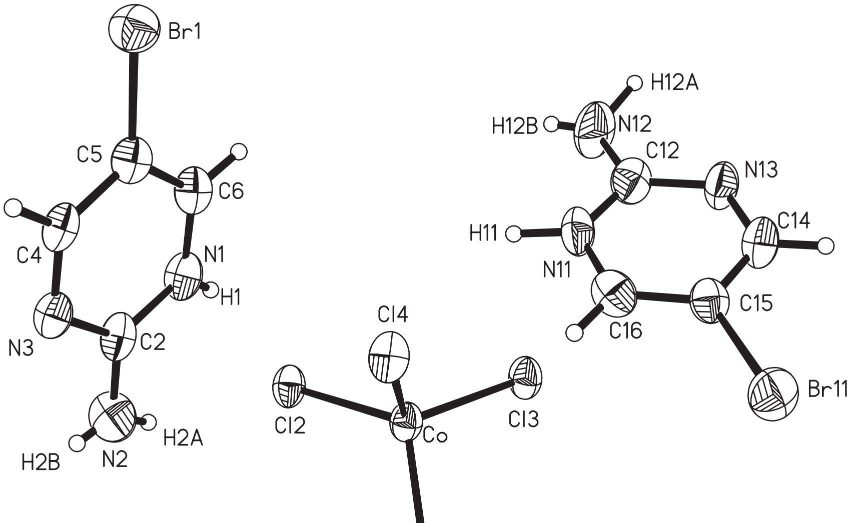

Figure 5. Thermal ellipsoid plot of **3** showing 50% probability ellipsoids. Hydrogens atoms are shown as spheres of arbitrary size and only those hydrogen atoms whose positions were refined are labeled.

$d_{Br11\cdots Cl4B} = 3.381(2)$ Å, $\perp\angle_{C15-Br11\cdots Cl4B} = 178.6(2)°$, $\angle_{Br1\cdots Cl3A-ZnA} = 102.3(2)°$; symmetry transformations: $A = x-1,\ y+1,\ z$; $B = -x+2,\ -y+1,\ -z$].

3.3. *Magnetic susceptibility*

Magnetic susceptibility data were collected for cobalt and manganese compounds **3**, **4**, and **5** in a 1000 Oe applied field over the temperature range 1.8–325 K (see figures 6–8, respectively). An additional data set was collected for **4** between 250 and 350 K (figure 7b) as a result of the upturn in the value of χT seen near room temperature

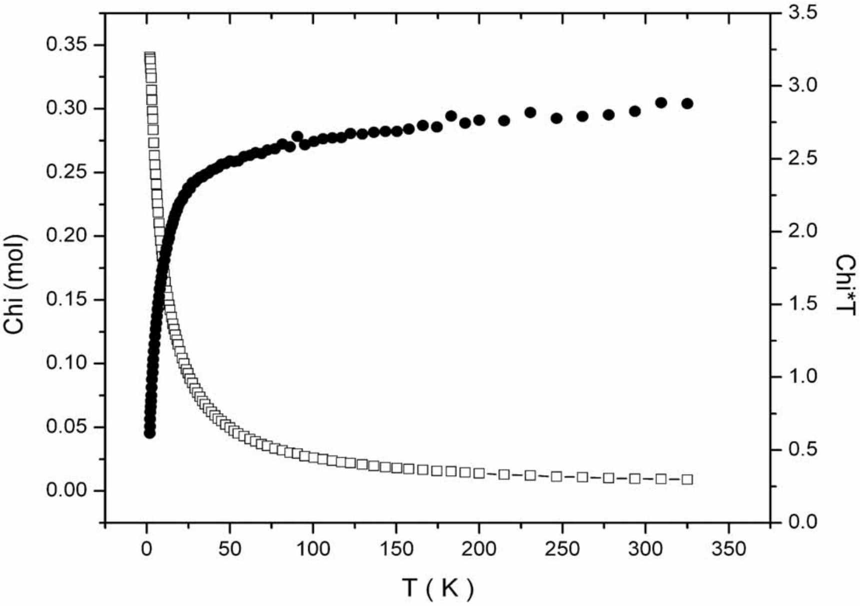

Figure 6. Magnetic susceptibility data for **3** collected at 1000 Oe [χ *vs*. T (□); χT *vs*. T (●)].

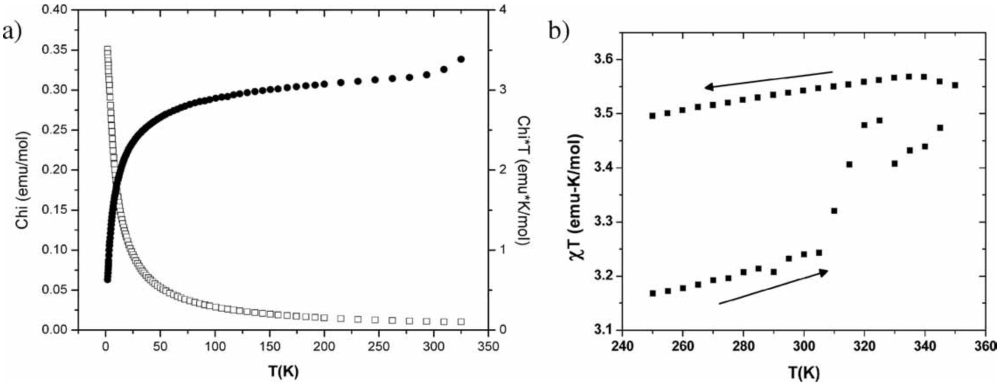

Figure 7. (a) Magnetic susceptibility data for **4** collected at 1000 Oe from 1.8 K to 325 K [χ *vs*. T (□); χT *vs*. T (●)]. (b) Magnetic susceptibility data for **4** collected at 1000 Oe from 250 K to 350 K.

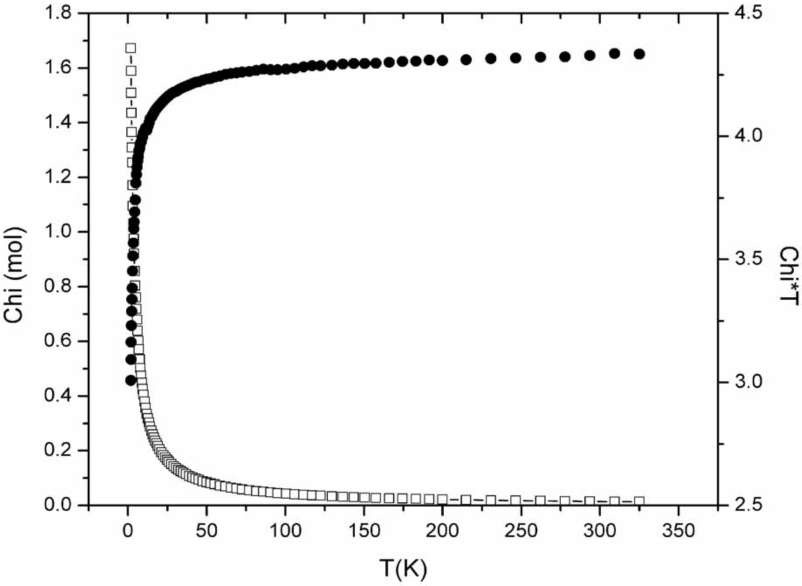

Figure 8. Magnetic susceptibility data for **5** collected at 1000 Oe [χ *vs*. T (□); χT *vs*. T (●)].

(see figure 7a). These data reveal a small maximum in the χT value near 320 K, but this is not reproducible when data is collected while decreasing the temperature (see discussion). No maxima are seen for any complexes in the χ *vs*. T data. The high temperature values of χT for the two cobalt complexes (300 K) are near 3.0 (**3**, 2.8; **4**, 3.2) as expected for a tetrahedral $S = 3/2$ ion exhibiting spin-orbit coupling. For the manganese complex, **5**, the value of 4.35 is in good agreement with the expected value of 4.4 for an $S = 5/2$ Heisenberg ion (that is, one with an isotropic internal field).

All three complexes show a rapid decrease in the value of χT below 50 K for the cobalt complexes and below 25 K for the manganese complex. A Curie-Weiss fit for the manganese complex **5** data gives a Weiss constant of $-1.20(1)$ K, suggesting very weak interactions.

3.4. *Infrared spectra*

All complexes show multiple absorptions in the 3500–3000 range due to N–H stretching vibrations. In **4**, these vibrations are broad, presumably due to adsorption of atmospheric moisture. The H–N–H scissoring motion (1649 cm^{-1} in the free ligand [24]) moves to higher energy in all complexes as expected upon protonation of the pyrimidine ring [1]. The out-of-plane H-bending vibration, near 792 cm^{-1} in the free organic, varies over ±20 cm^{-1}.

4. Discussion

The [$R_2^2(8)$] structural motif observed in both **1** and **3** (figure 2) is perhaps the most common feature in compounds of 2-aminopyrimidines and is seen in a variety of compounds when not inhibited by the presence of water molecules in the lattice [25].

Although the interplanar distance between adjacent dimers (3.13(1) Å) might indicate π-stacking interactions, the distance between the ring centroids (3.96(2) Å) and the ring slip angle (37.5(2)° between the plane of the ring and the inter-centroid vector) suggest that any such interaction is weak.

A second contributor to the stabilization of the lattice is the presence of halogen-halide contacts, that is, structural motifs of the form C–X···X′–M between organic halogen atoms and halide ions (in this case bonded to a metal ion). Lattice contacts have been shown to be significant in the synthesis of organic-based conductors [26] and in the synthesis of extended copper halide oligomers [27]. The interactions are characterized by X···X′ distances that are less than the sum of their van der Waals radii and nearly linear C–X···X′ angles [28]. These conditions are well met in the current compounds with Br···Cl distances ranging from 3.38–3.54 Å and C–Br···Cl angles ranging from 169–178°.

The $CoCl_4^{2-}$ anions pack in adjacent stacks with opposite orientations, and which form ladders via short Cl···Cl and Cl···Co contacts (see figure 9). The ladder rails are formed by close contacts of the form [2cf(3.81)] (for use of this nomenclature see Ref. [21]) between Cl1 and the adjacent $CoCl_4^{2-}$ ion related by a unit cell translation parallel to the *a*-axis [$d_{Cl1\cdots CoA} = 3.98$ Å; $d_{Cl1\cdots Cl2A} = 3.81$ Å; $d_{Cl1\cdots Cl4A} = 3.83$ Å]. Short Cl···Cl contacts between inversion related chloride ions (inversion center at 0, 0.5, 0.5) generate the ladder rungs [$d_{Cl2\cdots Cl2B} = 3.78$ Å]. Non-bonding contacts such as these have previously been observed to propagate weak antiferromagnetic exchange in copper complexes [29].

The inability to isolate metal complexes of 2-amino-5-bromopyrimidine is at first surprising considered the number of complexes known for 2-aminopyrimidine itself. To date, only two structures of metal complexes have been reported, one containing

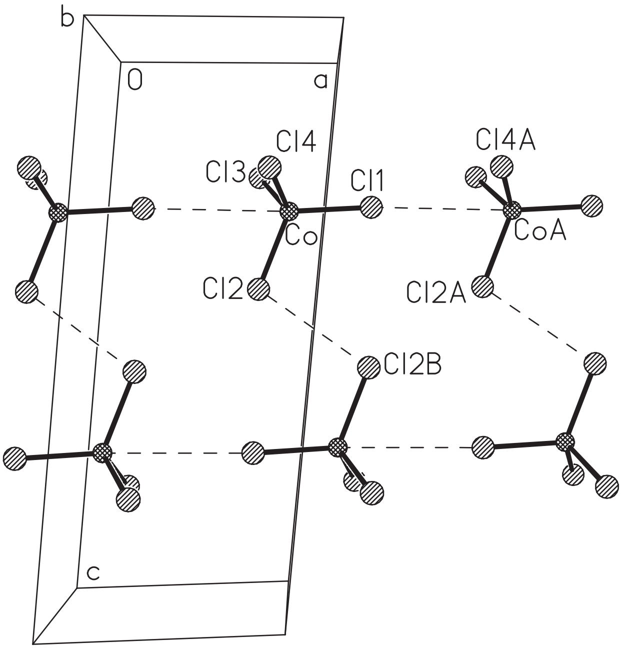

Figure 9. Packing structure for the $CoCl_4^{2-}$ anions in **3**. Dashed lines represent short interatomic distances.

Cu(II) [3] and one containing Cu(I) [14]. Under similar reaction conditions, only the salt, 2-abpmH$^+$X$^-$ was isolated. The addition of the 5-bromo substituent not only reduces the solubility of the compound in polar solvents, but also appears to reduce the basicity significantly. Only the strongly azophilic Cu ion coordinates in a variety of solvents and conditions.

The magnetic data for **3–5** are in agreement with weak antiferromagnetic exchange. In tetrahedral Co(II) complexes, a decrease in the χT product with decreasing temperature is expected due to single-ion anisotropy [30], however it should reach a minimum value of 1.7 at $T = 0$ K if the decrease in χT is due solely to single-ion effects. In both compounds, the value of χT at 1.8 K is well below that value (**3**, 0.45; **4**, 0.65) indicating the additional presence of antiferromagnetic exchange. The complexes are qualitatively the same below 300 K and the lack of a suitable model that incorporates both the single ion anisotropy and antiferromagnetic exchange prevents more detail interpretation. In the case of **5** and the Heisenberg ion Mn(II), there should be no single-ion anisotropy effects and the decrease in the value of χT at low temperatures may be attributed completely to antiferromangetic exchange. However, the value of θ_{CW} of $-1.20(1)$ K and the lack of an observed maximum in χ both indicate that the interactions are very weak. Attempts to fit the data to several models for low dimensional systems gave virtually indistinguishable results.

Above 300 K, the magnetic data for **4** exhibit hysteresis (see figure 7b). When data are collected in the warming mode, an abrupt increase in χT is seen beginning at 308 K followed by a small maximum near 320 K. A further increase in χT occurs up to the maximum tempearture of the data set (350 K). Upon cooling, a small maximum is observed just below 340 K followed by a smooth decrease in χT. The initial explanation for this was assumed to be due to the hygroscopic nature of the complex, causing decomposition of the sample. However, examination of the sample itself immediately after data collection showed no signs of the color change (blue to pink) observed upon hydration. [Note: Because the magnetic data are collected in a dry He atmosphere, the only potential source of water is the gelatin capsule itself. Degradation of the capsule and the associated color change from blue to pink were observed in samples left at room temperature for a few days]. The abrupt change in susceptibility observed at 308 K and the associated hysteresis suggest a structural phase change in the material. No changes in appearance were observed when a sample was heated on a Fisher-Johns hot-stage melting point apparatus.

Summary

The poor solubility of 2-amino-5-bromopyrimidine and its hydrohalide salts limits its use in the preparation of metal-organic salts. Tetrahalometallate complexes of Zn(II), Co(II), and Mn(II) with the 2-abpmH$^+$ cation have been successfully prepared, but attempts to prepare complexes of the free pyrimidine were unsuccessful. Crystal structure analysis shows the formation of head-to-tail dimers between the pyrimidinium ions as is common in 2-aminopyrimidine compounds. Magnetic data for the paramagnetic materials indicate that there are antiferromagnetic interactions between the tetrametallate ions, but that the interactions are weak in all cases. The apparent structural phase change observed in the magnetic data for (5-abpmH)$_2$CoBr$_4$ is being investigated further.

Acknowledgments

Financial support from the NSF (IMR-0314773) and The Kresge Foundation for the purchase of the SQUID magnetometer is gratefully acknowledged.

References

[1] J.-H.P. Lee, B.D. Lewis, J.M. Mendes, M.M. Turnbull, F.F. Awwadi. *J. Coord. Chem.*, **56**, 1425 (2003).
[2] M.E. Masaki, B.J. Prince, M.M. Turnbull. *J. Coord. Chem.*, **55**, 1337 (2002).
[3] B.J. Prince, M.M. Turnbull, R.D. Willett. *J. Coord. Chem.*, **56**, 441 (2003).
[4] (a) M. L. Richardson, M.F.G. Stevens. *J. Chem. Res., Synopses*, 482 (2002). (b) F. Berree, P. Girard-Le Bleis, B. Carboni. *Tetrahedron Lett.*, **43**, 4935 (2002).
[5] A.J. Whittle, J.J. Swanborough, D.R. Parry, A.J. Knee, R.L. Sunley. Brit. UK Pat. Appl. Application: GB 2002-21679.
[6] (a) W.J. Burgess, D. Jakas, W.F. Huffman, W.H. Miller, K.A. Newlander, M.A. Seefeld, I. Uzinskas, PCT Int. Appl. Application: WO 2002-US10332; (b) W.H. Miller, M.A. Seefeld, K.A. Newlander, I.N. Uzinskas, W.J. Burgess, D.A. Heerding, C.C.K. Yuan, M.S. Head, D.J. Payne, S.F. Rittenhouse, T.D. Moore, S.C. Pearson, V. Berry, W.E. DeWolf Jr, P.M. Keller, B.J. Polizzi, X. Qiu, C.A. Janson, W.F. Huffman. *J. Med. Chem.*, **45**, 3246 (2002).
[7] R.J. Sciotti, M. Pliushchev, P.E. Wiedeman, D. Balli, R. Flamm, A.M. Nilius, K. Marsh, D. Stolarik, R. Jolly, R. Ulrich, S.W. Djuric. *Bioorg. Med. Chem. Lett.*, **12**, 2121 (2002).
[8] J.J. Conde, W. Mendelson. *Tetrahedron Lett.*, **41**, 811 (2002).
[9] (a) G. Pujadas, J. Palau. *Protein Sci.*, **10**, 1645 (2001); (b) C. Alambra, J. Gao. *J. Comp. Chem.*, **21**, 1192 (2000).
[10] G. Smith, J.M. Gentner, D.E. Lynch, K.A. Byriel, C.H.L. Kennard. *Aust. J. Chem.*, **48**, 1151 (1995).
[11] G.A. van Albada, M.E. Quirox-Castro, I. Mutikainen, U. Turpeinen, J. Reedijk. *Inorg. Chim. Acta*, **298**, 221 (2000).
[12] G. Pon, R.D. Willett, B.A. Prince, W.T. Robinson, M.M. Turnbull. *Inorg. Chim. Acta*, **255**, 325 (1997).
[13] (a) T. Manfredini, G.C. Pellacani, A. Bonamartini-Corradi, L.P. Battaglia, G.G.T. Guarini, J.G. Giusti, G. Pon, R.D. Willett, D.X. West. *Inorg. Chem.*, **29**, 2221 (1990). (b) C. Zanchini, R.D. Willett. *Inorg. Chem.*, **29**, 3027 (1990).
[14] B.J. Prince, M.M. Turnbull. *J. Coord. Chem.*, **41**, 339 (1997).
[15] (a) M.J. Krische, J.-M. Lehn, N. Kyritsakas, J. Fischer, E.K. Wegelius, K. Rissanen. *Tetrahedron*, **56**, 6701 (2000). (b) M.J. Krische, J.-M. Lehn, N. Kyritsakas, J. Fischer. *Helv. Chim. Acta*, **81**, 1909 (1998).
[16] G.J. Cross, A.J. Seed, K.J. Toyne, J.W. Goodby, H. Hird, M. Carmen Artal. *J. Mat. Chem.*, **10**, 1555 (2000).
[17] *XSCANS, Version 2.0, Siemens Analytical X-ray Instruments*, 1993.
[18] *SHELXTL: v. 5.10, Structure Determination Software Suite, Sheldrick, G.M.*, Bruker AXS Inc., Madison, WI, 2001.
[19] G.M. Sheldrick, *SHELX97-2. Programs for the Solution and Refinement of Crystal Structures* University of Göttingen, Germany (1997).
[20] The structures have been deposited with the CCDC. Ref. numbers: **1**, 279453; **2**, 279452.
[21] M.M. Turnbull, C.P. Landee, B.M. Wells. *Coord. Chem. Rev.*, **249**, 2567 (2005).
[22] (a) R. Blachnik, H. Eickmeier, M. Gather, H. Reuter. *Z. Kristallogr.-New Cryst. Struct.*, **215**, 93 (2000). (b) A.S. Albrecht, C.P. Landee, M.M. Turnbull. *J. Chem. Cryst.*, **33**, 269 (2003). (c) C.R. Rice, S. Onions, N. Vidal, J.D. Wallis, M.-C. Senna, M. Pilkington, H. Stoeckli-Evans. *Eur. J. Inorg. Chem.*, 1985 (2002).
[23] M.C. Etter, J.C. MacDonald, J. Bernstein. *Acta Crystallogr., Sect. B*, **46**, 256 (1990).
[24] (a) M. Maehara, S. Nakama, Y. Nibu, H. Shimada, R. Shimada. *Bull. Chem. Soc. Jpn*, **60**, 2769 (1987). (b) E. Spinner. *J. Chem. Soc.*, 3119 (1962).
[25] (a) J. Scheinbeim, E. Schempp. *Acta Crystallogr., Sect. B*, **32**, 607 (1976). (b) P. Jensen, S.R. Batten, B. Moubaraki, K.S. Murray. *Chem. Commun.*, 793 (2000). (c) K.A. Byriel, C.H.L. Kennard, D.E. Lynch, G. Smith, J.G. Thompson. *Aust. J. Chem.*, **45**, 969 (1992). (d) V. Bertolasi, P. Gilli, V. Ferretti, G. Gilli. *Acta Crystallogr. Sect. B (Struct.Sci.)*, **57**, 591 (2001).
[26] H.M. Yamamoto, J. Yamaura, R. Kato. *J. Am. Chem. Soc.*, **120**, 5905 (1998).

[27] S. Haddad, F. Awwadi, R.D. Willett. *Cryst. Growth Des.*, **3**, 501 (2003).

[28] (a) M. Freytag, P.G. Jones, B. Ahrens, A.K. Fischer. *New J. Chem.*, **23**, 1137 (1999). (b) F.F. Awwadi, R.D. Willett, K.A. Peterson, B. Twamley, private communication.

[29] F.M. Woodward, A.S. Albrecht, C.M. Wynn, C.P. Landee, M.M. Turnbull. *Phys. Rev. B*, **65**, 144412 (2002).

[30] O. Khan, *Molecular Magnetism*, VCH Publishers, Inc, New York, (1993).